2021 43rd Annual International Conference of the
IEEE Engineering in Medicine & Biology Society (EMBC)
Oct 31 - Nov 4, 2021. Virtual Conference

Computational Modeling of Catheter-based Radiofrequency Renal Denervation with Patient-specific Model

Yan-Yan CHENG, Hong-Xing LIU, Meng ZHANG, You-Jun LIU, Qun NAN*

***Abstract*—Renal sympathetic denervation (RDN) is an effective approach for uncontrolled hypertension. Although several studies have compared the ablation characteristics at various locations, there is no direct comparative study on the effect of ablation in main and branch renal artery (RAs) and different electrode materials. The study aims to investigate the effect of different electrode materials (copper, gold, and platinum) and positions (proximal, middle, or distal site) on ablation. A 3D patient-specific renal artery model and a unipolar model (470 kHz) were constructed to mimic RDN. Two therapeutic strategies, including main (site 1 and 2) and branch (site 3) ablations were simulated with three electrode materials. The finite element method was used to calculate the coupled electric-thermal-flow field. Maximum lesion depth, width, area, and lesion angle were analyzed. The results showed that the difference in lesion width and depth was no mere than 0.5 mm, and the maximum difference value in lesion area is 0.683 mm^2 among three electrode materials. The lesion angle of proximal site 1 versus middle site 2 was 58.39 ° and 52.23 °, but the difference between distal site 3 and site 1, or site 2 was 29.19 ° and 35.35 ° respectively. There is no significant difference in the use of the three electrode materials, and ablation at the distal site of the artery is more effective.**

Keywords: **Renal sympathetic denervation; thermodynamic analysis; resistant hypertension; main RA ablation; branch RDN**

***Clinical Relevance*—This provides a reference for the selection of RF electrode materials and ablation locations.**

I. Introduction

Hypertension is a risk factor for chronic kidney disease, coronary heart disease, heart failure, and ischemic stroke, etc. [1]. More than three kinds of anti-pressure drugs cannot control the blood pressure level below 140/90 mmHg, which is called resistant hypertension (RH) [2]. This could greatly increase the risk of death. Renal sympathetic denervation (RDN) is currently an available option for the treatment of resistant hypertension (RH) [3]. In this method, the radiofrequency (RF) electrode is first punctured from the femoral artery to the renal artery through image guidance, and then RF ablation was performed directly on the artery wall. This approach uses RF energy generated by electrodes to disrupt the renal sympathetic nerve. Temperature exceeds 45–50 °C will cause irreversible nerve damage to neural tissue [4]. Therefore, it has great significance to evaluate the effectiveness and safety.

It has been confirmed that radiofrequency ablation (RFA) is currently an effective and safe treatment in the main renal artery (RA) [5]. However, clinical workers found that branch ablation may achieve more effective treatment because of its smaller diameter and closer to the nerves. Sakaoka A. et al [6]. confirmed the safety of branch RAs ablation by comparing the main RA ablation and branch RAs ablation in a porcine model. Michiel V. et al [7]. reported 97 patients and found that distal ablation placement effectively reduced blood pressure without any risk events. Henegar JR. et al [8]. found that RF-renal denervation lowered renal norepinephrine levels more significantly when performed in branches. A flow-up study of twenty-five patients [9] showed that combined association of the main domestic art and branches appears to improve BP lowering efficiency. Petrov. I. [10] et al. assessed an approach to percutaneous RDN for uncontrolled hypertension consisting of ablation of the primary branches (Y-pattern). Their study showed that brachial artery access was feasible and safe for RDN. Although several studies have compared the ablation characteristics of various locations, there is no direct comparative study on the effect of ablation in main and branch RAs and different electrode materials.

The study aims to investigate the ablation characteristics in different locations using different electrode materials (copper, gold, platinum). In this study, we constructed a patient-specific artery model and a single electrode to mimic RFA in three positions (proximal, middle, or distal site) and ablation with three electrode materials. Finally, the thermodynamic characteristics were analyzed, including thermal distribution, maximum lesion depth, width, area, and angle for quantitative analysis.

II. Materials and Methods

A. Model Construction

The construction process of a personalized model is shown in Fig. 1. Firstly, the original patient CT image (Fig. 1a) was selected, segmented, and transformed by Mimics software to obtain the geometric model of the left renal artery in STL format (Fig. 1b). To facilitate the selection of the inlet and outlet, it is necessary to surface the image in Geomagic Studio

*Research supported by the National Natural Science Foundation of China (31771021, 11832003) and the Jiangsu Science and Technology Project (BE2017758).

Qun NAN is with College of Life Science and Chemistry, Faculty of Environment and Life, Beijing University of Technology. Beijing, China (Correspondence author: fax: +86010-67392855; e-mail: nanqun@bjut.edu.cn).

Yan-Yan CHENG is with College of Life Science and Chemistry, Faculty of Environment and Life, Beijing University of Technology. Beijing, China (e-mail: 18865383172@163.com).

Hong-Xing LIU is with College of Life Science and Chemistry, Faculty of Environment and Life, Beijing University of Technology. Beijing, China (e-mail: hxliu1023@126.com).

Meng ZHANG with College of Life Science and Chemistry, Faculty of Environment and Life, Beijing University of Technology, (e-mail: 18601120075@163.com).

You-Jun LIU is with College of Life Science and Chemistry, Faculty of Environment and Life, Beijing University of Technology. Beijing, China (e-mail: lyjlma@bjut.edu.cn).

software and output the geometric model in IGS format (Fig. 1b). Finally, a patient-specific renal artery model (Fig. 1c) was established in COMSOL software. The total length of the renal artery was 60 mm. The length of the main artery is about 48.5 mm, and the length of the branch artery is 13.5 mm. The diameter of the main artery was about 6 mm to 12 mm respectively, and the range of the branch artery diameter was 7.10–7.50 mm. In addition, an abdominal cavity model (90 mm × 75 mm × 85 mm) served as a simulated external environment (Fig. 1d). The single electrode model was established to mimic RF ablation with a radius r of 0.62 mm and length h of 1.02 mm (Fig. 2) [14]. Table I lists the thermoelectric and fluid properties of these models [11][12].

The thermal and electrical conductivity of the tissue was temperature-dependent piecewise functions [13]. The thermal conductivity (k) increased linearly below 100 °C with a growth rate of 0.12%/°C. When the temperature exceeds 100 °C, k remained constant. The conductivity (σ) increases exponentially below 100 °C with an exponential growth rate of 1.5%/°C. Then σ was considered as four orders drop for T>100 °C to model the tissue desiccation process.

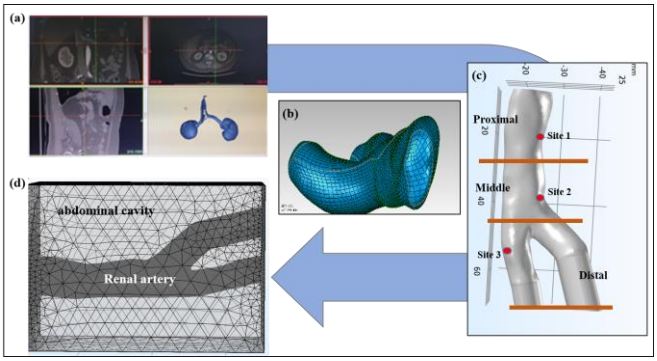

Figure 1. 3D renal artery models. (a) processed CT images, (b) optimized renal artery model, (c) geometric model, (d) mesh model.

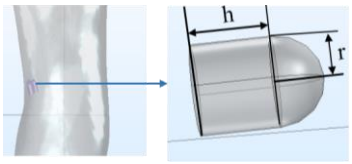

Figure 2. Geometric model of radiofrequency electrode.

TABLE I. MATERIALS PARAMETERS USED IN SIMULATION [11][12]

Material	ρ (kg/m^3)	σ (S/m)	C (J/kg·°C)	K (W/(m·°C)	μ (Pa·s)
Blood	1050	0.659	4180	0.54	0.0035
Abdominal cavity	1060	0.057	3600	0.212	-
Catheter	2250	0	1045	0.026	-
Gold-Au	317	4.5×10^7	129	401	-
Platinum-Pt	71	4×10^6	132	71	-
Copper-Cu	8700	5.998×10^7	385	400	-

B. Governing Equations

The Laplace equation (1) was used to calculate the electrical problem [15].

$$\nabla\cdot(\sigma(T)\nabla\mathbf{V})=0 \qquad (1)$$

where σ is the electrical conductivity (S/m), and $\mathbf{V}$ is voltage (V). The RF energy generated by RF heat source Q_r is calculated by $Q_r=\sigma|\mathbf{E}|^2$, and the vector electric field $\mathbf{E}$ is calculated by $\mathbf{E}=-\nabla V$.

In this study, there is a bidirectional thermal-flow coupled problem. Therefore, the incompressible Navier-Stokes equation works together with the Pennes heat transfer equation (Eq.2) [15]. The blood motion was taken into account to explain the loss of heat due to blood flow.

$$\rho c\frac{\partial T}{\partial t}=\nabla\cdot(k\nabla T)-Q_p+Q_m+Q_r-\rho c\mathbf{U}\cdot\nabla T \qquad (2)$$

where c_b is the specific heat capacity of the blood (J/(Kg·K)), T is the tissue temperature (°C), k is the thermal conductivity (W/(m·K)), t is time (s), Q_p is the heat loss caused by blood perfusion (W/m^3), Q_r is the heat source generated by RF power (W/m^3), Q_m is the metabolic heat generated by the tissue (W/m^3), and $\mathbf{U}$ is the blood velocity vector (m/s).

In the flow field, the blood flow was set as laminar compressible flow. The blood flow follows the conservation of mass (Eq.3), momentum (Eq.4), and energy (Eq. 5) [16].

$$\nabla\cdot(\rho\mathbf{U})=0 \qquad (3)$$

$$\frac{\partial(\rho\mathbf{U})}{\partial t}+\rho(\mathbf{U}\cdot\nabla)\mathbf{U}=\nabla\cdot[-p\mathbf{I}+\mu(\nabla\mathbf{U}+(\nabla\mathbf{U})^T]+\mathbf{F} \qquad (4)$$

$$\frac{\partial(\rho T)}{\partial t}+\nabla\cdot(\rho\mathbf{U}T)=\nabla\cdot\left(\frac{K}{c}\nabla T\right)+S_r \qquad (5)$$

where ρ is the density of the fluid (kg/m^3), P is the pressure (Pa), $\mathbf{I}$ is the normal stress (N), μ is the dynamic viscosity of the blood (Pa·s), $\mathbf{F}$ is the volume force vector (N/m^3), k is the thermal conductivity (W/m·K), c is the specific heat capacity of the liquid (J/(kg·K)), and S_r is the volumetric heat source (W/m^3).

C. Boundary conditions and Meshing Settings

In the whole model, all the outer surfaces of the tissue were grounded at zero current density. Set the initial potential value to 0V and apply a constant power of 8W to all electrodes for 60 s [17]. The blood flow in renal artery was considered to be an incompressible Newtonian fluid. The arterial wall was set as no wall slip. The average velocity in renal artery inlet was set as 0.4 m/s according to the literature measured [18], the outlet pressure was 0 Pa. Temperature of 37 °C was the initial temperature for renal artery and tissue. The tetrahedral mesh was used and refined at the interface of electrode and tissue (Fig. 1d). The mean number of mesh cells was 403865, the minimum mesh size was 0.05 mm, and the average mesh size was 0.67 mm. The initial solution time step was 1 s, and the solution time was set to 120 s for a finite element solution.

D. Thermal Injury Assessment of Lesion Zone

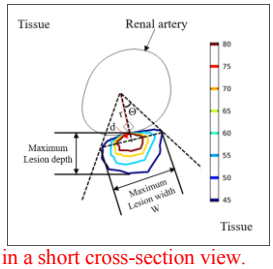

Figure 3. Lesion sizes in a short cross-section view.

The study used 45 °C as the effective treatment boundary. Figure 3 shows the evaluation of thermal injury sizes. It was

used to evaluate the thermal injury of the renal sympathetic nerves. The lesion angle of the renal artery can be calculated by Eq. 6.

$$Lesion\ Angle = \Theta = 2 \times tan^{-1}\left(\frac{\frac{1}{2} * W}{r + d}\right) \quad (6)$$

where Θ is the lesion angle (°), W is the maximum lesion width (mm), r is the lumen radius (mm), and d is the distance between maximum lesion width and artery wall (mm) (d_{site1}=0.74 mm, d_{site2}=0.78 mm, d_{site3}=0.76 mm).

III. Results and Discussions

In this study, the temperature distribution and lesion dimensions were obtained after various positions denervation with different electrode materials.

A. Lesion Size of Different Electrode Materials

As shown in Fig. 4, we can found that there was no significant difference in the maximum lesion depth, width, and area among the three electrode materials. The difference in lesion width and depth is less than 0.5 mm, and the maximum difference of ablation area is 0.683 mm^2. The highest temperature in tissues was 89.78 ℃ (Cu) > 86.70 ℃ (Au) > 83.19 ℃ (Pt).The reason for the above results is that the copper electrode has the largest electrical conductivity and thermal conductivity, followed by gold, and platinum was the smallest. But there is no significant difference in conductivity and thermal conductivity among them.

On the other hand, when using a copper electrode, the lesion width, depth, and area of branch ablation compared to main RA increased by 2.26 mm, 1.06 mm, and 9.49 mm^2, respectively, increased by 2.26 mm, 1.04 mm, and 10.50 mm^2 for a gold electrode, and increased by 1.96 mm, 0.72 mm, and 10.26 mm^2 for a platinum electrode. The lesion sizes at the branch RA are larger than those at the main RA under the same electrode materials. Therefore, we select copper materials for the next thermal injury analysis of various locations.

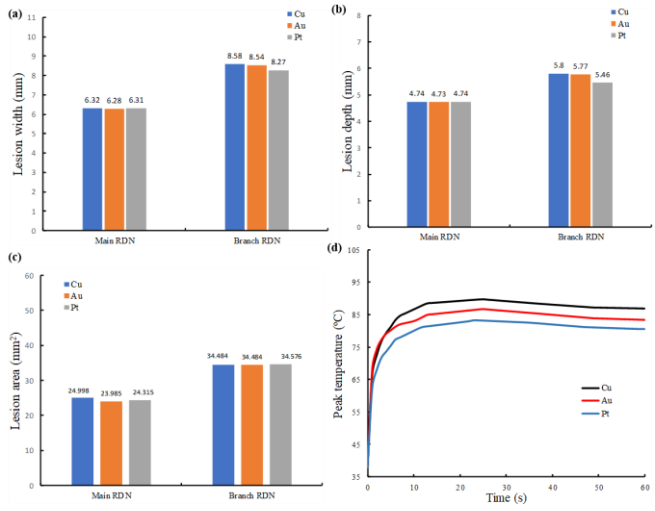

Figure 4. Comparison of lesion size. (a) lesion width, (b) lesion depth, (c) lesion area, and (d) peak temperature.

B. Thermal Injury in Various Locations

It can be found that the lesion sizes in the proximal site 1 and the middle site 2 is smaller than the distal segment treatment (Fig. 5), and the values are given in Table II.

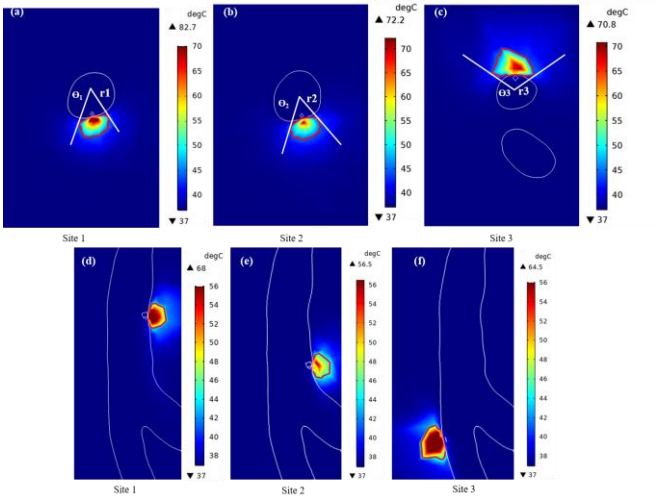

Figure 5. Temperature distribution at different ablation locations.

TABLE II. Lesion Sizes at Different Locations

Location	Renal Dimeter (mm)	Lesion depth (mm)	Lesion width (mm)	Lesion area (mm^2)	Lesion angle Θ (°)
Proximal (Site 1)	9.83	4.74	6.32	25.00	58.39
Middle (Site 2)	10.72	4.36	6.02	20.93	52.23
Distal (Site 3)	7.43	5.80	8.58	34.49	87.58

The reason for the above results can be explained as that compared with the main RA (diameter=9.83 mm), the diameter of the branch (diameter =7.43 mm) is smaller. It assumed that the cross-sectional diameter of the two branches is approximately equal. The flow velocity at the inlet is about 0.4 m/s and the mean flow velocity at the main RA (site 1) is about 0.29 m/s. According to the principle of conservation, the mean flow velocity at the branch RA (site 3) is about 0.25 m/s calculated by Eq. 7. Smaller velocity will reduce the cooling effect of blood and electrode and avoid the loss of RF energy, which will increase the lesion depth.

$$v_1 A_1 = v_2 A_2 + v_3 A_3 \quad (7)$$

where v_1 is the velocity of the main RA, v_2 and v_3 are the velocity in the bifurcation RAs (m/s), A is the cross-sectional area of blood flow (m^2).

C. Tissue and blood temperature in Various Locations

The highest temperature in the tissue still appears in the distal ablation. The temperature distributions from blood center to tissue of the three positions increase with distance in the near-field (<1 mm) and decrease with distance in the far-field (Fig. 6). Besides, there was no significant difference in the temperature between 60 and 120 s for single electrode ablation because the difference of each position was no more than 2 ℃.

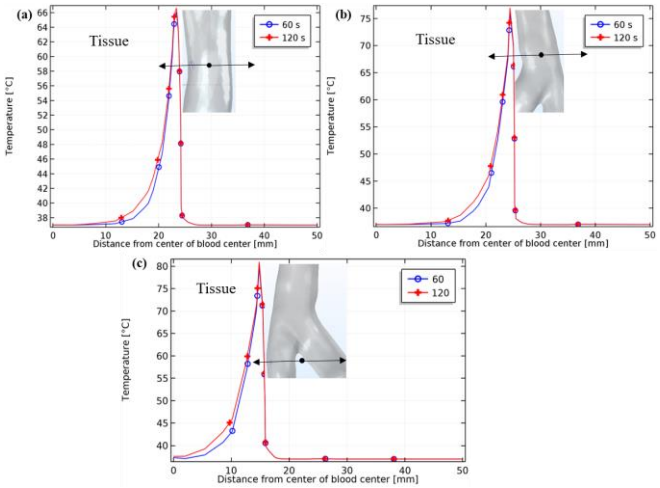

Figure 6. Temperature distribution at different ablation locations. (a) Site1, (b) Site 2, and (c) Site 3.

D. Fluid field change after RDN in Various Locations

To observe the flow field changes after ablation, the velocity distribution in the longitudinal section was obtained (Fig. 7). The results show that compared with normal blood flow, it caused higher flow velocity change in the branch (site 3) ablation. The maximum velocity after ablation increased by 0.07 (site 1), 0.08 (site 2), and 0.10 m/s (site 3), respectively compared with no ablation.

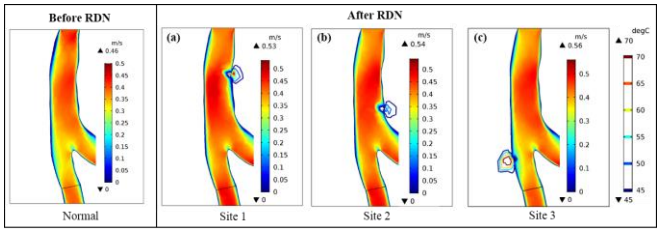

Figure 7. 2D velocity distribution and effective lesion distribution.

IV. Conclusion

In this study, a thermodynamics analysis was conducted after renal denervation based on a patient-specific model. The effects of different electrode materials and positions on ablation were analyzed. The numerical results showed that there is no significant difference using copper, gold, and platinum electrodes to perform RF ablation. However, the lesion size was significantly affected by the different ablation sites (main and branch RA) under the same electrode material. Because the renal nerves are close to the branch RAs, a deeper lesion depth may damage more renal sympathetic nerves. Therefore, performing ablation in the branch or the main combined branch RAs is more effective. But, it caused higher temperature change and flow velocity change. The limitation is that the renal arterial model established in this study does not include the vascular wall. Whether it will cause greater thermal damage to the vascular wall or greater hemodynamic changes such as branch stenosis need to be further studied.

Acknowledgment

This work was supported by the National Natural Science Foundation of China (31771021, 11832003), and Beijing International Science and Technology Cooperation Base for Intelligent Physiological Measurement and Clinical Transformation.

References

[1] E. J. Benjamin, M. J. Blaha, S. E. Chiuve, et al, "Heart disease and stroke statistics-2017 Update: a report from the American Heart Association," Circulation, vol. 135, no. 10, pp. E146–E603, 2017.

[2] N. L. Sun, "Evaluation and treatment of resistant hypertension," *Chinese Journal of practical medicine*. vol. 39, no. 01, pp. 8-10, 2019.

[3] M. P. Schlaich, P. A. Sobotka, H. Krum, et al, "Renal denervation as a therapeutic approach for hypertension: novel implications for an old concept," *Hypertension*, vol. 54, no. 6, pp. 1195–1201, 2009.

[4] E. J. Berjano, "Theoretical modeling for radiofrequency ablation: state-of-the-art and challenges for the future," *Biomed. Eng. Online*, vol. 5, no. 1, pp. 24-24, 2006.

[5] S. I. AI. Raisi, J. Pouliopoulos, J. Swinnen, et al, "Renal Artery Denervation in Resistant Hypertension: The Good, The Bad and The Future," *Heart Lung Circ.*, vol. 29, no. 1, pp.94-101, 2020.

[6] A. Sakaoka, S. D. Rousselle, H. Hagiwara, et al, "Safety of catheter-based radiofrequency renal denervation on branch renal arteries in a porcine model," *Catheter. Cardiovasc. Interv.*, vol. 93, no. 3, pp.494-502, 2018.

[7] M. Beeftink, W. Spiering, V. Michiel, et al, "Renal denervation beyond the bifurcation: The effect of distal ablation placement on safety and blood pressure," *J. Clin. Hypertens.*, vol. 19, no. 4, pp.371-378, 2017.

[8] J. R. Henegar, Z. Yongxing, H. Cary, et al, "Catheter-Based Radiofrequency Renal Denervation: Location Effects on Renal Norepinephrine," *Am. J. Hypertens.*, vol. 28, no. 7, pp.909-914, 2015.

[9] K. Fengler, S. Ewen, R. Hllriegel, et al, "Blood Pressure Response to Main Renal Artery and Combined Main Renal Artery Plus Branch Renal Denervation in Patients with Resistant Hypertension," *J. Am. Heart Assoc.*, , vol. 6, no. 8, 2017.

[10] I. Petrov, I. Tasheva, I. Garvanski, et al, "Comparison of standard renal denervation procedure versus novel distal and branch vessel procedure with brachial arterial access," *J. Am. Coll. Cardiol.*, vol. 20, no. 1, pp. 38-42, 2018.

[11] D. Schutt, E. J. Berjano, D. Haemmerich, "Effect of electrode thermal conductivity in cardiac radiofrequency catheter ablation: A computational modeling study," *Int. J. Hyperthermia*, vol. 25, no.2, pp.99-107, 2009.

[12] T. Dong, Q. Nan, Y. Y. Cheng, et al, "Radiofrequency ablation of renal sympathetic nerve: Numerical simulation and ex vivo experiment," *Adv. Mech. Eng.*, vol. 10, no. 6, pp. 1–11, 2018.

[13] M. Trujillo, E. Berjano, "Review of the mathematical functions used to model the temperature dependence of electrical and thermal conductivities of biological tissue in radiofrequency ablation," *Int. J. Hyperthermia*, vol. 29, no. 6, pp. 590-597, 2013.

[14] S. I. AI Raisi, J. Pouliopoulos, M. T. Barry, et al, ".Evaluation of lesion and thermodynamic characteristics of Symplicity and EnligHTN renal denervation systems in a phantom renal artery model," *Eurointervention*, vol. 10, no. 2, pp. 277-284, 2014.

[15] A. González-Suárez, E. Berjano, "Comparative Analysis of Different Methods of Modeling the Thermal Effect of Circulating Blood Flow During RF Cardiac Ablation," *IEEE Trans. Biomed. Eng.*, vol. 63, no.2, pp.250-259, 2016.

[16] T. L. Bergman, A. S. Lavine, F. P. Incropera, et al, "Fundamen-tals of heat and mass transfer," in *Hoboken*, 6th ed. NJ: Wiley, 2006.

[17] X. M. Guo, F. Zhai, Q. Nan, "The temperature field simulation of radiofrequency catheter-based renal sympathetic denervation for resistant hypertension," *Bio-Med. Mater. Eng.*, vol. 24, no.1, pp. 315-321, 2014.

[18] B. L. Dong, X. M. Hou, "Ultrasonic murement of Renal Aretrial Dimeter and Blood Flow Index in Normal Individuals," *Chinese J. ultrasound imaging*, vol. 3, no. 2, pp. 87-89, 1994.